Molecular Crystals and Liquid Crystals

Publication details, including instructions for authors and subscription information:
http://www.tandfonline.com/loi/gmcl20

PHASE DIAGRAM OF NAPHTHALENE AND N-PENTACOSANE: EXPERIMENTAL DETERMINATION

P. M. Ghogomu [a], R. Rakotosaona [b], M. Bouroukba [b], D. Petitjean [b], N. Hubert [b] & M. Dirand [b]

[a] Department of Inorganic Chemistry, Faculty of Science, University of Yaounde 1., P. O. Box 812, Yaounde, Cameroon

[b] Laboratoire de Thermodynamique des Milieux Polyphasés, Ecole Nationale Supérieure des Industries Chimiques, Institut National Polytechnique de Lorraine, 1 rue Grandville, BP 451, 54001 Nancy Cédex, France

Version of record first published: 15 Jul 2010

To cite this article: P. M. Ghogomu, R. Rakotosaona, M. Bouroukba, D. Petitjean, N. Hubert & M. Dirand (2004): PHASE DIAGRAM OF NAPHTHALENE AND N-PENTACOSANE: EXPERIMENTAL DETERMINATION, Molecular Crystals and Liquid Crystals, 408:1, 103-115

To link to this article: http://dx.doi.org/10.1080/15421400490425892

Mol. Cryst. Liq. Cryst., Vol. 408, pp. 103–115, 2004

ISSN: 1542-1406 print/1563-5287 online
DOI: 10.1080/15421400490425892

Taylor & Francis
Taylor & Francis Group

PHASE DIAGRAM OF NAPHTHALENE AND N-PENTACOSANE: EXPERIMENTAL DETERMINATION

P. M. Ghogomu
Department of Inorganic Chemistry, Faculty of Science, University of Yaounde 1., P. O. Box 812, Yaounde, Cameroon

*R. Rakotosaona, M. Bouroukba, D. Petitjean, N. Hubert, and M. Dirand**
Laboratoire de Thermodynamique des Milieux Polyphasés, Ecole Nationale Supérieure des Industries Chimiques, Institut National Polytechnique de Lorraine, 1 rue Grandville, BP 451, 54001 Nancy Cédex, France

The phase diagram of (naphthalene + n-pentacosane) has been determined by thermometrical and differential thermal analyses and X-ray diffraction carried out on the two pure compounds and twelve binary mixtures. The solids phases of the pure compounds are immiscible, but there is cosolubility in the liquid state. With increasing temperature, the binary mixtures undergo structural changes corresponding to those of pure n-pentacosane, while naphthalene seems to retain its initial crystalline structure until fusion occurs. The binary diagram, determined by experiments, displays an eutectic solidification with immiscibility in the solid state:

$$\text{liquid} \leftrightarrow \delta_o\text{-}C_{10}H_8 + \beta'_o(\text{Pbnm})\text{-}C_{25}H_{52}.$$

Keywords: phase diagram; calorimetry; n-pentacosane; naphthalene; X-ray diffraction

INTRODUCTION

One of the continuing challenges in understanding the physico-chemical and thermodynamic behavior of paraffinic crude oils and their distillates at low temperatures has been to establish the structure-property relationships among the linear n-alkane (hereafter denoted by C_n) homologues susceptible to precipitating as wax [1–21]. However, between such waxes,

*Corresponding author. E-mail: mdirand@ensic.u-nancy.fr

or between simple or multicomponent C_ns and naphtenes, aromatics, and/or asphaltenes present in oil, a number of interesting properties certainly must exist. In particular, knowledge of the thermodynamic properties of systems containing polycyclic aromatics and long-chain C_ns is important in numerous petroleum industrial applications. Studying such systems may be considered as a first step towards a thermodynamic description of heavy petroleum fractions. Wax formation problems have mainly been handled on the basis of empirical models and, more recently, on the development of new thermodynamic models. Those models unfortunately face the serious problem of scarcity of experimental data on the thermodynamic and structural behavior of multicomponent systems, indispensable for their validation. Also, the complexity of such systems makes it difficult to explain and exploit the structural and thermal behaviors observed.

It is in this light that we decided to investigate the thermal and structural behavior of mixtures of normal-pentacosane (n-$C_{25}H_{52}$) and naphthalene ($C_{10}H_8$). Some studies have been carried out on similar systems [22–29]. In this article, we present the temperatures of the solid–solid transition and fusion of the twelve binary mixtures. The structural evolution of the mixtures with temperature is also given. The phase diagram of this system is proposed.

EXPERIMENTAL PART

Normal-pentacosane C_{25} (FLUKA) and naphthalene ($C_{10}H_8$) (FLUKA) had mole fraction purities of over 0.98 and 0.99, respectively, as determined by gas chromatography. In order to obtain a mixture the pure solid components were weighed in the adequate proportions, melted and mixed carefully, then quenched in a crystallizing dish maintained at very low temperature in a Dewar vessel filled with liquid air. A uniform concentration of the components in the mixture was thus ensured. The solidified mixture was ground to a fine powder and stored at room temperature.

Calorimetric studies were carried out using a coupled simple thermal analysis (STA)–differential thermal analysis (DTA) device constructed in this laboratory. It consists of a stainless steel crucible closed by a screw stopper. A thermocouple hermetically sealed through a hole in the stopper was kept in contact with the sample. The crucible was introduced into a programmable furnace oven equipped with cooling and heating elements based on the Peltier effect, allowing it to work from 240.15 K to 373.15 K. The cold junction was carried out with the same type of thermocouple (T-type copper/copper-nickel) with the opposite poles and it was immersed in a water-ice bath at 273.15 K. The temperature signal was recorded on a SEFRAM 8201 recorder connected to a computer used for

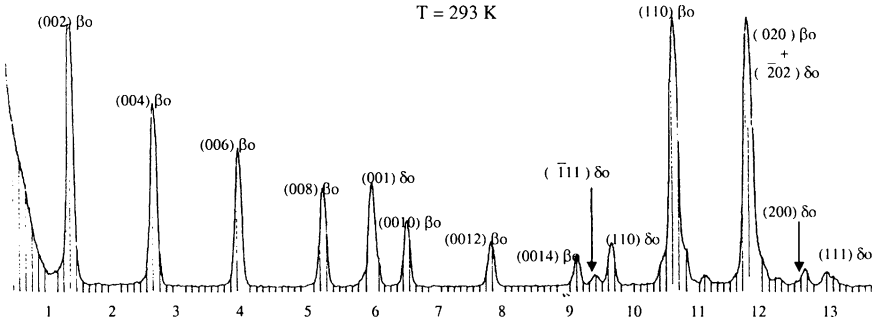

FIGURE 1 XRD pattern (λK_α copper) of the mixture (0.49 of naphthalene + 0.51 of n-pentacosane); Observation of the characteristic X-lines of the structure of each pure compound (β_0-C_{25} and δ_0-$C_{10}H_8$).

the rapid analysis of the thermograms. The sample was first heated until melted and then slowly cooled. The actual measurement then began, by heating the sample at a rate of 1 K/min. The plot of the heating curve versus time gives the solid-state transition temperature (where applicable) and the melting temperature. All measurements were carried out at thermodynamic equilibrium with increasing temperature to avoid any supercooling phenomenon. Our study included temperatures from 293.15 K to 373.15 K. The uncertainty on the observed temperatures was estimated to be ± 0.1K.

X-Ray diffractometry (XRD) was carried out on samples at 293.15, 308.15, 317.15, 321.15, 328.15, and 338.15 K. This was done using powder samples and a λK_α copper radiation in a Theta 60 CGR diffractometer. The sample holder was heated by the Peltier effect, and this enabled the examination of the sample at different temperatures with an accuracy of ± 0.2 intensity of the $(0\,0\,\ell)$ diffraction lines (Figures 1 and 2). A focused monochromatic beam with a filament intensity of 10 mA and 48 kV was used, and the line positions were measured with an accuracy of $\pm 0.025°$ for each Bragg angle value.

Structural Behavior of the Pure Components

Naphthalene ($C_{10}H_8$)

The room temperature crystalline structure of naphthalene was determined by Chanh and Haget-Bouillaud [30], and it is monoclinic with the crystallographic space group $P2_1/a$. The unit-cell parameters are $a = 0.8259$ nm, $b = 0.598$ nm, $c = 0.8668$ nm, $Z = 2$, and $\beta = 122{,}6°$ [49]. It is hereafter denoted $\delta_0(P2_1/a)$-$C_{10}H_8$. All Bragg's diffraction lines with intensity greater than 10% are detected.

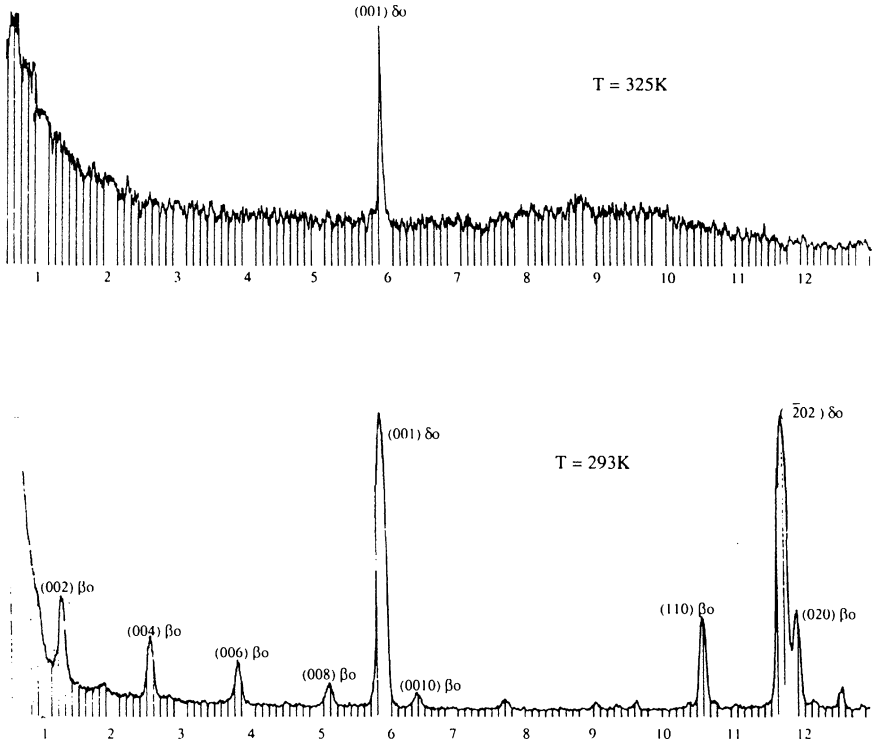

FIGURE 2 Structural behavior of the mixture (0.8 of naphthalene + 0.2 of n-pentacosane) versus temperature at 293 K there is observation of the two solid phases (β_0-C_{25} and δ_0-$C_{10}H_8$). When the temperature is equal to 325 K, all the diffraction lines of the β_0-C_{25} phase disappear. The diffusion halo situated between the angles from 7° to 11° (λK_α copper) and the line (0 0 1) δ_0 indicate the presence of the liquid phase and the δ_0-$C_{10}H_8$ solid phase, respectively.

As the temperature increases, the characteristic diffractions retained their respective positions. X-ray diffraction was carried out on the pure compound at 284.65 K, 311.95 K, 319.85 K, and 333.65 K. Our observations show that naphthalene does not undergo any phase change before melting in equilibrium conditions.

n-pentacosane (C_{25})

The C_n crystallographic structures of 'low temperature' solid phases have been specified by Craig et al. [31] and Chevallier et al. [32], who have respectively clarified the crystallographic space groups and the correlations between the crystalline long c-parameter and the number of carbon atoms

of pure C_ns. At low temperatures, the crystalline structure of the odd-numbered C_ns is orthorhombic with the crystallographic space group Pbcm [30], hereafter denoted as β_o(Pbcm).

The structural behavior of odd-numbered C_ns, as a function of temperature, has been the subject of numerous publications, particularly concerning C_{25} [33–50]. Concerning this C_n, Ungar [43], Snyder et al. [45], and Robles et al. [46] observed the following sequence, reported by Chevallier et al. [42]:

$$C_{25}\beta_o(\text{Pbcm}) \xrightarrow{\delta} \beta'_o(\text{Pbcm}) \xrightarrow{\gamma} \text{B(Aa)} \xrightarrow{\text{o-d}} \beta(\text{Fmmm}) \Rightarrow \beta\text{–RI(Fmmm)} \rightarrow \alpha\text{–RII(R}\bar{3}\text{m)} \rightarrow \text{Liquid},$$

where $\rightarrow$ denotes first-order transitions and $\Rightarrow$ denotes higher-order transitions.

Order–order transitions

δ-transition [45]: According to Nozaki et al. [50], this solid–solid transition leads to the orthorhombic (ordered) phase, denoted β'_o(Pbnm).

γ-transition: A second order–order transition was observed by Piesczek et al. [40], Ungar [43], and Robles et al. [46]. It corresponds to the appearance of a monoclinic phase, called B, with the crystallographic space group, called Aa [47–49]. However, like other authors [35,36,40,41] Chevallier et al. [42], who studied the effects of impurities on the solid–solid transition temperatures of the odd-numbered homologous C_ns from eicosane up to nanocosane, did not observe the γ-transition in a very high purity synthetic sample of C_{25}.

Order–disorder transition. This solid–solid transition, which gives a major thermal effect below fusion, corresponds to the appearance of the disordered orthorhombic β(Fmmm) phase [11,33,35,36,42–44]. Hereafter this order–disorder transition is denoted as o–d transition. When temperature increases, the molecules of this β(Fmmm) phase are driven by a movement of the 'Rotator' type denoted RI; this phenomenon, which is observed at varying temperatures for pure C_{25}, does not correspond to a first-order transition according to Gibb's law but to a higher order transition [34,36].

Disorder–disorder transition. Just below the melting point, the last solid–solid transition is observed in C_{25} with the appearance of the rhombohedral α-RII(R$\bar{3}$m) Rotator phase [11,33–36,38,42–44] at the temperature equal to 322.6 K [46].

RESULTS AND DISCUSSION

In order to determine the behavior of the mixtures ($C_{10}H_8 + C_{25}$) as a function of the concentration and the temperature, and thus to establish the binary phase diagram, we used the experimental techniques of the thermodynamic (STA, DTA) and structural (X-ray diffraction) characterization that have been already described in other literature [2–10,33–38].

Structural Behavior of the Mixtures at Room Temperature (T = 293.15 K)

Twelve mixtures ($C_{10}H_8 + C_{25}$), whose concentrations are given in Table 1, were studied by X-ray diffraction at 293.15 K. In all of the diffraction experiments, the characteristic diffraction lines of the structure of each pure compound (β_0(Pbcm)-C_{25} and δ_0(P2$_1$/a)-$C_{10}H_8$) were observed separately. Their relative intensities evolved as a function of the ratio of each component in the two-phase mixture, and those evolutions are observed on the XRD patterns obtained for the mixtures whose $C_{10}H_8$ mole fractions are equal, respectively, to 0.49 (Figure 1) and 0.8 (Figure 2). They particularly concern the X-ray diffraction lines (0 0 ℓ) of the β_0-C_{25} phase and ((0 0 1) and ($\overline{2}$ 0 2)) of the δ_0-$C_{10}H_8$ phase, whose intensities increase with the $C_{10}H_8$ mole fraction (Figures 1 and 2, T = 293 K). These observations confirm that the two compounds are not miscible at the solid state in the range of the studied concentrations, and they form a two-phase region whatever the studied composition (Figure 3).

Thermal Behavior

Pure naphthalene seems to show no solid-state transition: only the melting peak was registered by STA and DTA at a temperature equal to 354.05 ± 0.1 K, close to the value of 354 K recorded in literature [39].

Like numerous authors [35,36,38,40–42], we observed two solid–solid transitions before the fusion of C_{25}:

δ transition β_0(Pbcm) → β'_0(Pbnm) at $T_\delta = 311.9 \pm 0.1$ K
o-d transition β'_o(Pbnm) → β(Fmmm) at $T_{o\text{-}d} = 320.75 \pm 0.1$ K

However, we did not register the γ solid-state transition below the o–d transition as was reported in other literature [43–46]; this transition may be mixed with the o–d transition peak or may not be present as a result of the high purity of C_{25} that we used, as mentioned by Chevallier et al. [42]. For C_{25}, the sequence of transitions and phases is as follows:

TABLE 1 Structural Evolutions Versus T Temperature and x Mole Fraction of C_{25}

T/x		T_δ/K		T_E/K		T_{o-d}/K		T_{fus}/K
$C_{10}H_8$	δ_0		δ_0			δ_0		354.05
0.036	$\delta_0+\beta_0$(Pbcm)	311.95	$\delta_0+\beta'_o$(Pbnm)	318.65		δ_{0+}L		350.65
0.085	$\delta_0+\beta_0$(Pbcm)	311.85	$\delta_0+\beta'_o$(Pbnm)	318.65		δ_{0+}L		348.65
0.144	$\delta_0+\beta_0$(Pbcm)	311.95	$\delta_0+\beta'_o$(Pbnm)	318.85		δ_{0+}L		345.15
0.268	$\delta_0+\beta_0$(Pbcm)	311.85	$\delta_0+\beta'_o$(Pbnm)	318.85		δ_{0+}L		336.75
0.308	$\delta_0+\beta_0$(Pbcm)	311.85	$\delta_0+\beta'_o$(Pbnm)	318.95		δ_{0+}L		321.45
0.356	$\delta_0+\beta_0$(Pbcm)	311.85	$\delta_0+\beta'_o$(Pbnm)	318.95		δ_{0+}L		319.05
0.426	$\delta_0+\beta_0$(Pbcm)	311.95	$\delta_0+\beta'_o$(Pbnm)	318.95	β'_o(Pbnm) + L	320.65	β(Fmmm) + L	320.85
0.524	$\delta_0+\beta_0$(Pbcm)	311.85	$\delta_0+\beta'_o$(Pbnm)	318.95	β'_o(Pbnm) + L	320.85	β(Fmmm) + L	322.15
0.593	$\delta_0+\beta_0$(Pbcm)	311.95	$\delta_0+\beta'_o$(Pbnm)	318.85	β'_o(Pbnm) + L	320.75	β(Fmmm) + L	323.35
0.675	$\delta_0+\beta_0$(Pbcm)	311.85	$\delta_0+\beta'_o$(Pbnm)	319.05	β'_o(Pbnm) + L	320.75	β(Fmmm) + L	324.85
0.768	$\delta_0+\beta_0$(Pbcm)	311.85	$\delta_0+\beta'_o$(Pbnm)	319.05	β'_o(Pbnm) + L	320.75	β(Fmmm) + L	325.45
0.874	$\delta_0+\beta_0$(Pbcm)	311.95	$\delta_0+\beta'_o$(Pbnm)	319.05	β'_o(Pbnm) + L	320.75	β(Fmmm) + L	326.65
$C_{25}H_{52}$	β_0(Pbcm)	311.9	$\delta_0+\beta'_o$(Pbnm)		β'_o(Pbnm)	320.75	β(Fmmm)	327.05

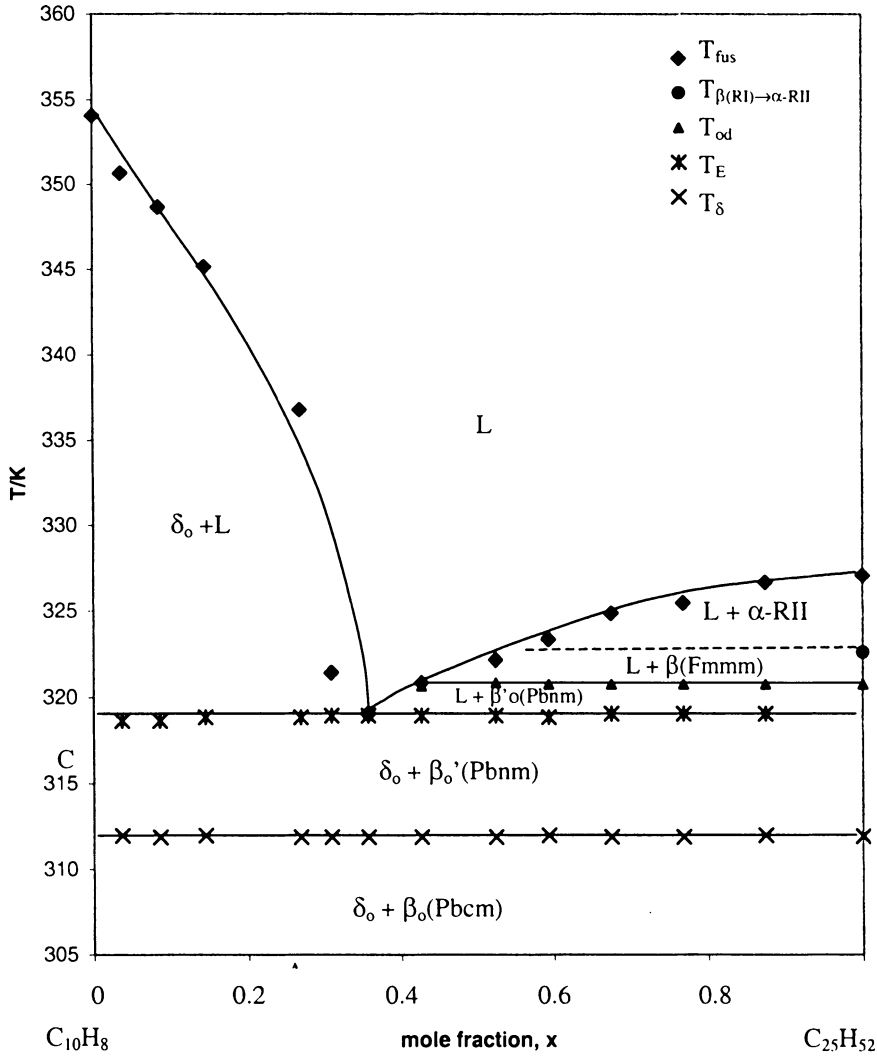

FIGURE 3 Phase diagram of the binary system (naphthalene + n-pentacosane).

$$\beta_0(\text{Pbcm})\text{-}C_{25} \xrightarrow{\delta} \beta_0'(\text{Pbnm}) \xrightarrow{\text{o-d}} \beta(\text{Fmmm}) \Rightarrow \beta\text{-RI(Fmmm)}$$
$$\rightarrow \alpha\text{-RII}(R\bar{3}m) \xrightarrow{\text{fusion}} \text{liquid},$$

where $\rightarrow$ denotes first-order transition and $\Rightarrow$ higher order transition.

Two thermal behaviors were observed by simple and differential thermal analyses of the mixtures as a function of the x molar fraction of C_{25}.

1. $0 \leq x < 0.356$ molar fraction of C_{25}: with increasing temperature, two peaks were observed above the δ transition of C_{25}. The first peak appeared at a constant temperature (on average $T \approx 318.9 \pm 0.5\,K$) whatever x molar fraction, and the second peak at a temperature that decreased in function with the increasing x molar fraction of C_{25} (Table 1) from 0 up to 0.356. This temperature points to the fusion end (liquidus temperature), T_{fus}.
2. $0.356 < x \leq 1$ molar fraction of C_{25}: like with the mixtures before, above the δ transition of C_{25}, the first peak appeared at a constant temperature $T \approx 318.9 \pm 0.5\,K$ whatever x C_{25} molar fraction. Next a second peak, whose intensity increased against C_{25} molar fraction, also at a constant temperature corresponding to the o–d transition temperature of C_{25} $T_{o-d} \approx 320.75\,K$, and finally a third peak whose temperature increased with the rise of the C_{25} molar fraction from 0.426 up to 1 (Table 1). This temperature shows the liquidus point of the fusion end, T_{fus}.

Structural Behavior with Increasing Temperature

As for pure C_{25}, the structural δ transition β_0(Pbcm)-$C_{25} \rightarrow \beta'_0$(Pbnm) was observed in all the mixtures at constant temperature (on average, $T \approx 311.9 \pm 0.5\,K$) by X-ray diffraction, according to the depictions of Jouti et al. [35] and Chevallier et al. [42]. The X-ray diffraction observations show that below the δ transition temperature ($T_\delta = 311.9 \pm 0.5\,K$) the mixtures display two solid phases that correspond to the two pure compounds δ_0-$C_{10}H_8$ and β_0(Pbcm)-C_{25}, and in the temperature range set between $T_\delta = 311.9\,K$ and $T = 318.9\,K$ the two phases that coexist are δ_0-$C_{10}H_8$ and β'_0(Pbnm)-C_{25}.

As shown by differential thermal analyses, two structural behaviors were observed by X-ray diffraction at $T \approx 318.9 \pm 0.5\,K$.

1. Naphthalene-rich side ($0 \leq x < 0.356$ C_{25} molar fraction): all of the characteristic X-diffraction lines of the β_0(Pbnm)-C_{25} phase disappeared, while those of δ_0-$C_{10}H_8$ retained their positions (Figure 2).
2. C_{25}-rich side ($0.356 < x \leq 1$ C_{25} molar fraction): conversely, with these all of the characteristic X-diffraction lines of δ_0-$C_{10}H_8$ disappeared, while those of β'_0(Pbnm)-C_{25} were retained.

In the two cases above, the disappearance of one of the two solid phases comes with the appearance of the liquid. The observation of an invariant temperature of start fusion (on average $T_E = 318.9 \pm 0.5\,K$) in all the binary mixtures correspond to the following eutectic fusion:

$$\text{liquid} \leftrightarrow \delta_0(P2_1/a)\text{-}C_{10}H_8 + \beta'_0(\text{Pbnm})\text{-}C_{25}$$

Above the eutectic temperature ($T_E = 318.9 \pm 0.5\,K$) there is a coexistence with the binary.

1. Liquid and solid δ_0-$C_{10}H_8$ phases on the naphtalene-rich side: on the XRD pattern of Figure 2, carried out at 325 K for the mixture with a molar fraction of $C_{10}H_8$ equal to 0.8, the characteristic lines of the β_0-C_{25} phase disappeared and only the peaks of δ_0-$C_{10}H_8$ phase are observed, particularly the line (0 0 1) with a diffusion halo corresponding to the presence of the liquid phase (Figure 2, $T = 325\,K$).
2. Liquid and solid β'_0(Pbnm)-C_{25} phases on the C_{25}-rich side: the β'_0(Pbnm)-C_{25} phase underwent the o–d transition at $T_{o-d} = 320.75 \pm 0.5\,K$ as the pure C_{25}; above the o–d transition temperature the mixtures displayed the liquid and solid β-RI (Fmmm) orthorhombic Rotator phases and then the liquid and solid α-RII ($R\bar{3}m$) rhombohedral Rotator phases above $T \approx 322.6\,K$, as observed by Robles et al. [46]. All of the characteristic structural evolutions, observed by X-ray diffraction in the course of the solid–solid transitions, were identical to those already described by Jouti et al. [35].

CONCLUSION

The thermodynamic and structural experimental results are summarized in Table 1 and lead to the binary diagram ($C_{10}H_8$:C_{25}) shown in Figure 3. This diagram displays no miscibility in the solid phases of two pure compounds with eutectic solidification as observed in other systems, for instance:

Binary diagrams: n-alkane + n-alkane, where the difference of the length of molecules is too high [17,36,51–57]; n-alkane + nonlinear hydrocarbon (aromatic or cyclic) [5,12–19,25–28,58]; tris (hydroxymethy amino-methane + pentaglycerine [59] or naphthalene + 2-R-naphthalene with R = F,Cl,Br,SH,CH_3 [39].

Ternary diagrams: two consecutive heavy n-alkanes + light hydrocarbons solvent [5,18,19].

Pseudobinary multicomponent systems: paraffinic wax + light hydrocarbon [9,36,58].

NOMENCLATURE

δ_0 monoclinic structure of the solid phase of naphthalene

β_0(Pbcm) orthorhombic structure of the C_{25} ordered phase at room temperature

β'_0(Pbnm) orthorhombic structure of the C_{25} ordered phase above the δ-transition temperature

β(Fmmm) orthorhombic structure of the C_{25} disordered phase; this phase displays the rotator state, β-RI, when the temperature increases

$\alpha(R\bar{3}m)$. rhombohedral structure of the C_{25} second disordered rotator phase

L liquid

T_δ/ K temperature of δ-transition of C_{25}: $\beta_0(Pbcm) \Longleftrightarrow \beta'_0(Pbnm)$

T_E/ K eutectic temperature: liquid $\leftrightarrow \delta_0$-$C_{10}H_8 + \beta'_0$(Pbnm)-$C_{25}H_{52}$

T_{o-d}/ K temperature of ordered $\leftrightarrow$ disordered transition of C_{25}: $\beta'_0(Pbnm) \leftrightarrow \beta(Fmmm)$

T_α/ K temperature of the disordered-disordered transition of C_{25}: β-RI(Fmmm) $\leftrightarrow \alpha$-RII($R\bar{3}m$)

T_{fus}/ K temperature of melting-end

REFERENCES

[1] Luth, M., Nyburg, S. G., Robinson, P. M., & Scott, A. (1974). *Mol. Cryst. Liq. Cryst., 27*, 337–341.

[2] Hasnaoui, N., Dellacherie, J., Schuffenecker, L., Dirand, M., & Balesdent, D. (1988). *J. Chim. Phys., 85*(2), 153–156.

[3] Jouti, B., Petitjean, D., Provost, E., Bouroukba, M., & Dirand, M. (1995). *J. Mol. Struct., 356*, 191–194.

[4] Dirand, M., Achour, Z., Jouti, B., Sabour, A., & Gachon, J. C. (1996). *Mol. Cryst. Liq. Cryst., 275*, 293–303.

[5] Goghomu, P. M., Dellacherie, J., & Balesdent, D. (1989). *J. Chem. Thermodyn. 21*, 295–298.

[6] Dirand, M., Chevallier, V., Provost, E., Bouroukba, M., & Petitjean, D. (1998). *Fuel, 77*, 1253–1257.

[7] Chevallier, V., Provost, E., Bourdet, J. B., Bouroukba, M., Petitjean, D., & Dirand, M. (1999). *Polymer, 40*, 2121–2128.

[8] Chevallier, V., Petitjean, D., Bouroukba, M., & Dirand, M. (1999). *Polymer, 40*, 2129–2137.

[9] Chevallier, V., Bouroukba, M., Petitjean, D., Dirand, M., Pauly, J., Daridon, J. L., & Ruffier-Meray, V. (2000). *Fuel, 79*, 1743–1750.

[10] Chevallier, V., Briard, A. J., Petitjean, D., Hubert, N., Bouroukba, M., & Dirand, M. (2000). *Mol. Cryst. Liq. Cryst., 350*, 273–291.

[11] Dirand, M., Bouroukba, M., Briard, A. J., Chevallier, V., Petitjean, D., & Corriou, J. P. (2002). *J. Chem. Thermodyn., 34*, 1255–1277.

[12] Ghogomu, P. M., Bouroukba, M., Dellacherie, J., Balesdent, D., & Dirand, M. (1997). *Thermochimica Acta, 306*, 69–72.

[13] Ghogomu, P. M., Schuffenecker, L., Dellacherie, J., Dirand, M., & Balesdent, D. (1997). *Thermochimica Acta, 294*, 147–155.

[14] Ghogomu, P. M., Bouroukba, M., Dellacherie, J., Balesdent, D., & Dirand, M. (1997). *Thermochimica Acta, 302*, 159–164.

[15] Ghogomu, P. M., Bouroukba, M., Dellacherie, J., Balesdent, D., & Dirand, M. (1997). *Thermochimica Acta, 302*, 151–158.

[16] Ghogomu, P. M., Provost, E., Bouroukba, M., Dirand, M., & Hoch, M. (1998). *J. Thermal Analysis, 53*, 49–56.
[17] Provost, E., Chevallier, V., Bouroukba, M., Petitjean, D., & Dirand, M. (1998). *J. Chem. Eng. Data, 43*, 745–749.
[18] Provost, E., Balesdent, D., Bouroukba, M., Petitjean, D., Ruffier-Meray, V., & Dirand, M. (1999). *J. Chem. Thermodyn. 31*, 1135–1149.
[19] Floter, B., Hollanders, B., de Loos, T. W., & De Swaan Arons, A. J. (1997). *J. Chem. Eng. Data, 42*, 562–563.
[20] Daridon, J. L., Xans, P., & Montel, F. (1996). *Fluid Phase Equilibria, 117*, 241–244.
[21] Jouti, B., Bouroukba, M., Balesdent, D., & Dirand, M. (1998). *J. Therm. Anal., 54*, 785–788.
[22] Choi, P. B. & McLaughlin, E. (1983). *Ind. Eng. Chem. Fundam., 22*, 46–49.
[23] Choi, P. B., Williams, C. P., Buehring, K/G., & McLaughlin, E. (1985). *J. Chem. Eng. Data, 30*, 403–406.
[24] Djordjevic, M. (1991). *Thermochimica Acta, 177*, 109–112.
[25] Aoulmi, A., Bouroukba, M., Solimando, R., & Rogalski, M. (1995). *Fluid Phase Equilibria, 110*, 283–287.
[26] Mahmoud, R., Solimando, R., & Rogalski, M. (1998). *Fluid Phase Equilibria, 148*, 139–146.
[27] Mahmoud, R., Rogalska, E., Solimando, R., & Rogalski, M. (1999). *Thermochimica Acta, 325*, 119–124.
[28] Mahmoud, R., Solimando, R., Bouroukba, M., & Rogalski, M. (2000). *J. Chem. Eng. Data, 45*, 433–436.
[29] Domanska, U., Lachwa, J., Morawski, P., & Malanowski, S. (1999). *J. Chem. Eng. Data, 44*, 974–984.
[30] Chanh, N. B. & Haget-Bouillaud, Y. (1972). *Acta Cryst., B28*, 3400–3404.
[31] Craig, S. C., Hastie, G. P., Roberts, K. J., & Sherwood, J. N. (1994). *J. Mater. Chem., 4*, 977–980.
[32] Chevallier, V., Petitjean, D., Ruffier-Meray, V., & Dirand, M. (1999). *Polymer, 40*, 5953–5956.
[33] Doucet, J., Denicolo, O., Craievich, A. F., & Germain, C. (1984). *J. Chem. Phys., 80*, 1647–1651.
[34] Jouti, B., Bourdet, J. B., Bouroukba, M., & Dirand, M. (1996). *Mol. Cryst., Liq. Cryst., 270*, 159–173.
[35] Jouti, B., Bourdet, J. B., Petitjean, D., Bouroukba, M., & Dirand, M. (1996). *Mol. Cryst., Liq. Cryst., 287*, 275–283.
[36] Dirand, M., Bouroukba, M., Chevallier, V., Petitjean, D., Behar, E., & Ruffier-Meray, V. (2002). *Chem. Eng. Data, 47*, 115–143.
[37] Nouar, H., Bouroukba, M., Petitjean, D., & Dirand, M. (1998). *Mol. Cryst., Liq. Cryst., 309*, 273–282.
[38] Nouar, H., Petitjean, D., Bouroukba, M., & Dirand, M. (1999). *Mol. Cryst., Liq. Cryst., 326*, 381–391.
[39] Van Duijneveldt, J., Chanh, N. B., & Oonk, H. A. J. (1989). *Calphad, 13*(1), 83–89.
[40] Maroncelli, M., Qi, S. P., Strauss, H. L., & Snyder, R. G. (1982). *J. Am. Chem. Soc., 104*, 6237–6247.
[41] Sirota, E. B., King, J. R., Suiger, D. M., & Shao, H. H. (1993). *J. Chem. Phys., 98*, 5809–5824.
[42] Chevallier, V., Bouroukba, M., Petitjean, D., Barth, D., Dupuis, P., Benoist, L., & Dirand, M. (2001). *J. Chem. Eng. Data, 46*, 1114–1122.
[43] Ungar, G. (1983). *J. Phys. Chem., 87*, 689–692.
[44] Ungar, G. & Masic, J. (1985). *J. Chem. Phys., 89*, 1036–1042.

[45] Snyder, R. G., Maroncelli, M., Qi, S. P., & Strauss, H. L. (1981). *Sciences, 214*, 188–192.
[46] Robles, L., Mondieg, D., Haget, Y., & Cuevas-Diarte, M. A. (1998). *J. Chim. Phys., 95*, 92–96.
[47] Ewen, B., Fisher, E. W., Piesczek, W., & Strobl, G. R. *J. Chem. Phys., 197*(461), 5265–5272.
[48] Piesczek, W., Strobl, G. R., & Malzahu, K. (1974). *Acta Crystallogr., B30*, 1278–1288.
[49] Strobl, G., Ewen, B., Fisher, E., & Piesczek, W. (1974). *J. Chem. Phys., 61*, 5257–5264.
[50] Nozaki, K., Higashitani, N., Yamamoto, T., & Hara, T. (1995). *J. Chem. Phys., 103*, 5762–5766.
[51] Haget, Y. (1993). *J. Chim. Phys., 90*, 313–324.
[52] Turner, W. R. (1971). *Ind. Eng. Chem., Prod. Res. Dev., 10*, 238–260.
[53] Petitjean, D., Pierre, M., Ghogomu, P., Bouroukba, M., & Dirand, M. (2002). *Polymer, 43*, 345–349.
[54] Dorset, D. L. (1986). *Macromolecules, 23*, 623–633.
[55] Dorset, D. L. (1986). *Macromolecules, 19*, 2965–2974.
[56] Basson, I. & Reynhardt, E. C. (1992). *Chem. Phys. Lett., 198*, 367–372.
[57] Srivastava, S. P., Butz, T., Oschmann, H. J., & Rahimian, I. (2000). *Pet. Sci. Technol., 18*, 493–518.
[58] Dorset, D. L. (1997). *J. Phys. Chem., B 101*, 4870–4874.
[59] Barrio, M., Font, J., Lopez, D. O., Muntassel, J., Tamarit, J. L., Negrier, Ph., Chanh, N. B., & Haget, Y. (1991). *Les Equilibres entre Phases, XVIII JEEP*, ed. Legendre, B. (Chatenay-Malabry).